Processing and properties of porous TiNbTaZr alloy for biomedical applications using the powder metallurgy route

by Aris Widyo Nugroho

Processing and properties of porous TiNbTaZr alloy for biomedical applications using the powder metallurgy route*

AW Nugroho
Department of Mechanical Engineering, Curtin University, Perth, Western Australia, Australia;
Department of Mechanical Engineering, Muhammadiyah University of Yogyakarta, Indonesia

G Leadbeater† and IJ Davies
Department of Mechanical Engineering, Curtin University, Perth, Western Australia, Australia

ABSTRACT: *Titanium alloys, due to their biocompatibility and low stiffness, are among the most studied of metallic implant materials. Whereas most titanium-based biomaterials are produced from pre-alloyed powders, in this work the authors have utilised elemental powder to manufacture porous TiNbTaZr alloys using a powder metallurgy technique based on the pressurised gas-induced expansion of pores. Samples of porous TiNbTaZr alloy were prepared from a blend of elemental powders sealed into steel cans under a pressurised argon atmosphere. Following this, the pressurised cans were densified by hot isostatic pressing (HIP) at 1100 °C and 100 MPa for 4 hours, with cubic specimens from each can being treated in a vacuum furnace (1100, 1225, 1350 °C) for 10 hours in order to allow the pressurised pores to expand due to creep of the surrounding metal (foaming). Following this, the phase composition of HIP and foamed samples was characterised by x-ray diffraction (XRD), while microstructure and pore morphology were examined using optical microscopy and scanning electron microscopy. Mechanical testing under compressive loading was carried out at a strain rate of 10^{-3} s^{-1}. Following HIP, XRD indicated the suppression of peaks related to α-Ti while microstructural analysis revealed the particle boundaries to have become diffuse due to the partial dissolution of Nb and Ta, with initial porosity levels being generally less than 3 %. Increasing the foaming temperature led to increases in porosity and proportion of α-Ti phase with a resulting decrease in elastic stiffness. These porous materials were concluded to be an attractive candidate for low stiffness biocompatible implant materials.*

1 INTRODUCTION

Porous metals are known to exhibit significant advantages in a wide variety of applications due to their low density and novel physical, mechanical, thermal, electrical and acoustic properties (Ashby et al, 2000). These materials have already shown potential for lightweight structures, thermal management, energy absorption and more recently for biomedical applications. However, costs associated with manufacture are often the main limitation to increasing the scope of applications. While porous aluminium has been fabricated commercially at reasonable cost, this form of aluminium exhibits relatively low strength and performs poorly under high temperature operation. Thus, the fabrication of other porous metal alloys with a high specific strength, such as those based on titanium, has been an area of particular interest in recent years. Titanium

* Paper originally presented at the 6th Australasian Congress on Applied Mechanics (ACAM6), 12-15 December 2010, Perth, Western Australia.

† Corresponding author Garry Leadbeater can be contacted at g.leadbeater@curtin.edu.au.

holds significant promise for biomedical applications since it is known to be a biocompatible, while the introduction of porosity may reduce the stiffness to match that of bone (10-40 GPa) (Long & Rack, 1998), thus reducing the stress shielding effect. In addition to this, the porous structure may have the potential to entrap specific proteins such as vitronectin and fibronectin in order to promote osteoblastic cell attachment, proliferation and differentiation on the implant surface, thus allowing the completion of bone ingrowth into the implant and leading to improvements in implant fixation. The majority of titanium implant materials contain alloying elements in order to obtain appropriate mechanical properties. However, adverse body reaction to some of the most commonly utilised alloying elements such as aluminium (Perl & Brody, 1980) and vanadium (Rae, 1981), together with higher than preferred stiffness levels for the porous structure, have been noted (Oppenheimer, 2007).

It has been established that the ideal titanium-based implant material should have high strength but commensurate stiffness with that of human bone. For example, Song et al (1999) suggested that β stabilising elements such as Nb, Ta and Zr can simultaneously increase strength and decrease the elastic modulus for titanium alloys. In addition, these particular alloying elements are known to possess low toxicity and interact well with neighbouring cells (Eisenbarth et al, 2004). Studies have found that β titanium alloys offer lower elastic moduli than those of pure titanium and α-β titanium alloys (eg. Ti-6Al-4V) commonly used as load bearing orthopaedic implant materials (Niinomi, 1998). For example, Niinomi and colleagues have developed Ti-29Nb-13Ta-4.5 alloy with an elastic modulus of 67 GPa (Hao et al, 2002), compared to a typical value of 120 GPa for pure titanium. Therefore, porous biomedical titanium alloys based on these β stabilising elements, ie. Ti, Nb, Ta and Zr, have been under extensive investigation.

Due to the high chemical reactivity and high melting point of titanium, a solid state foaming process is preferable rather than liquid foaming in order to produce porous titanium alloy. However, sintering of loose powder is known to generally produce a structure with low porosity (Oh et al, 2003) whereas foaming using a polymer space holder raises concerns due to contamination from the polymer during its removal (Jee et al, 2000). Another solid state foaming technique, first developed by Kearns et al (1987), has achieved promising results with porosity levels reported up to 44% (Murray & Dunand, 2004). This technique utilises highly pressurised argon pores created by the hot isostatic pressing (HIP) of metal powders, such as commercially pure Ti powder (Murray & Dunand, 2004) and Ti-6Al-4V pre-alloyed powder (Oppenheimer, 2007; Kearns et al, 1987), in the presence of argon gas and followed by expansion of the pressurised argon at high temperature. The level of porosity achieved can be controlled by the foaming parameters, such as argon pressure, foaming time or foaming temperature.

A significant disadvantage of this method, however, is the use of pre-alloyed powder, which adds to the cost and complexity of the manufacturing route. A much simpler and lower cost procedure would be to use elemental powders as the starting materials but concerns have been raised regarding whether alloying can be completed under the conditions required to manufacture highly porous foam. Therefore, the purpose of the present study was to fabricate porous titanium alloys from biocompatible elemental powders, ie. Ti, Nb, Ta and Zr, that possessed high strength and low elastic modulus using a powder metallurgy method and argon filled pore expansion.

2 EXPERIMENTAL PROCEDURE

The starting elemental powders employed in this work, namely Ti, Nb, Ta and Zr (CERAC Inc., Milwaukee, USA), were weighed to produce the nominal composition as presented in table 1.

The elemental powders were found to be angular in morphology, with a wide distribution of particle sizes below 44 μm. The powder was initially mixed in a roller mixer with the morphology of the mixed powders being presented in figure 1. The Ta particles appear brightest due to their high atomic number and they are followed by Nb, Zr and Ti.

Approximately 50 g of the mixed powder was placed into stainless steel cans with an inner diameter and length of 28 and 30 mm, respectively. Each can was

Table 1: Powder composition used for the alloys.

	Nb	Ta	Zr	Ti
Weight %	29.04	13.02	4.51	Balance
Purity %	99.8	99.9	99.7	99.5

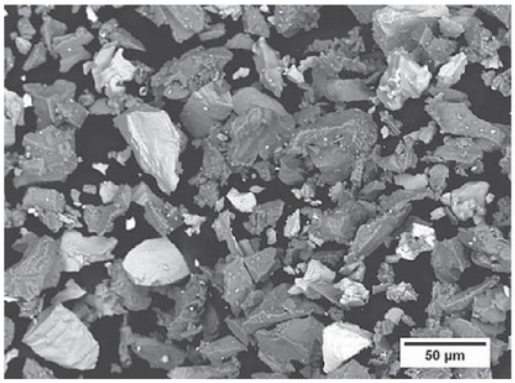

Figure 1: Backscattered scanning electron micrograph of the mixed powder.

subsequently evacuated to approximately 10^{-2} Pa and then backfilled with argon gas and sealed. The pressurised cans were then densified using HIP at 1100 °C for 4 hours under 100 MPa of argon at the Australian Nuclear Science and Technology Organisation. Cube specimens of approximate side dimension 10 mm were cut from the centre of each HIP billet using an electrical discharge machine (EDM). Following this, the cubic specimens were foamed in an argon flushed graphite element vacuum furnace (10^{-2} Pa) at a temperature of 1150, 1225 or 1350 °C for 10 hours and then furnace cooled to room temperature.

Following this foaming process, the cubic specimens were cut into flat plates using EDM for characterisation purposes. Prior to observation using x-ray diffraction and microscopy, the EDM damage layer and foamed surface layer were removed by light grinding and polishing and followed by ultrasonic cleaning in acetone. Phase identification within the specimens was carried out using a Bruker D8 Advance x-ray diffractometer (XRD) with CuKα radiation under conditions of 40 kV and 40 mA. Following phase identification, the specimens were mounted into epoxy resin and polished to a 1 μm surface finish prior to examination using a Nikon Eclipse ME600 optical microscope and a Zeiss Evo 40XVP scanning electron microscope. The fraction of porosity within each specimen was determined by image analysis of 20 micrographs for each specimen using open source software (ImageJ, National Institutes of Health, USA). Compression tests were carried out on specimens of dimension 4 × 4 × 8 mm (similar in size to that previously used by Erk et al (2008)) using an Instron 5500R mechanical testing machine at a strain rate of 10^{-3} s^{-1}. The specimen strain was measured using two clip gauges attached to the platen surfaces in contact with the specimen.

3 RESULTS AND DISCUSSION

The composition and change in phases during fabrication of the specimens were examined by XRD with typical XRD patterns for the initial mixed powder, densified powder following HIP and following foaming at 1100, 1225 and 1350 °C shown in figure 2. The XRD pattern for the initial mixed powder (figure 2(a)) indicated the presence of both hexagonal (hcp), ie. alpha titanium, alpha zirconium, and isomorphous body centered cubic (bcc) structures, ie. niobium and tantalum.

Following HIP at 1100 °C for 4 hours, the XRD pattern (figure 2(b)) showed peaks related to α-titanium to have been suppressed and unobservable whereas peaks corresponding to isomorphous bcc structures, ie. tantalum, niobium and β-titanium, were clearly observed. This result indicates that dissolution of tantalum and alpha titanium, together with niobium as a beta nucleating agent, was still not complete

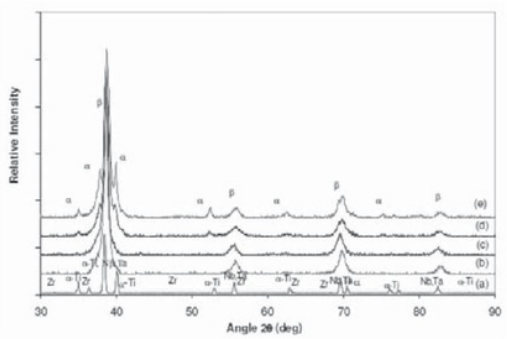

Figure 2: X-ray diffraction patterns for various samples – (a) mixed powder, (b) densified powder by HIP at 1100 °C, and foamed at (c) 1100 °C, (d) 1225 °C and (e) 1350 °C.

following HIP. In addition, α-titanium particles had been transformed to β-titanium and this was attributed to the HIP temperature of 1100 °C having been higher than the β transition temperature (883 °C for pure titanium). Furthermore, it is known that the presence of isostatic stress through the HIP procedure may induce retention of the β-titanium phase during furnace cooling to room temperature. As a comparison, Taddei et al (2004) reported that sintering of beta alloy powders at 1100 °C without the presence of stress and followed by furnace cooling resulted in peaks attributed to α phase being observed due to transformation from the β phase during cooling. Thus, the HIP procedure was considered to have noticeably improved beta phase development. Interestingly, peaks related to zirconium were not detected within the HIP and foamed samples with this phenomenon also being noted in previous studies (Taddei et al, 2004; Sakaguchi et al, 2004).

The XRD patterns of the samples foamed at 1100, 1225 and 1350 °C show the presence of peaks corresponding to β phase, with only minor peaks being noted in relation to α phase. Of interest, the relative intensities of the α peaks become higher with increasing foaming temperature. It is known that the ratio of XRD peak height between the strongest peaks of the constituent phases can be used to estimate their volume fraction (Hao et al, 2002) and therefore the height ratio of the (0111)α to (110)β peaks indicated that the volume fraction of α phase increased with foaming temperature. This result was explained by the following interpretation, namely that in a highly β-stabilised alloy, elemental composition affects the phase transformation during heating and cooling. A higher content of Nb is known to reduce the martensite formation temperature, even possibly down to room temperature, so that martensite-α structure formation may be suppressed (Tang et al, 2000). Furthermore, the addition of zirconium in a quaternary alloy may reduce the critical cooling

rate, thus allowing β phase to be retained during furnace cooling from 1100 °C to room temperature (Tang et al, 2000). At higher foaming temperatures, a longer time to reach room temperature would be required, thus allowing greater intrusion into the β+α phase field. In accordance with the continuous cooling transformation diagram proposed by Tang et al (2000), a higher volume fraction of β phase may transform to α phase, while a very small portion of β phase may transform to ω phase. While none of the foamed samples indicated the presence of ω phase by XRD, this may simply be due to the low amount of ω phase present being below the detection threshold for XRD (Ikeda et al, 2002; Banumathy et al, 2009).

Microstructures of the HIP sample and the sample foamed at 1100 °C have been shown in figure 3. The backscattered scanning electron micrograph of the specimen HIP at 1100 °C for 4 hours (figure 3(a)) showed the presence of titanium particles (dark), niobium (grey) and tantalum (bright). This micrograph also revealed that the particle boundaries had become diffuse due to the dissolution of niobium and partial dissolution of tantalum particles, indicating that for this HIP condition, homogenisation of the alloy was still incomplete. The HIP specimens were found to contain pores (black spots) that were attributed to incomplete dissolution between the elemental powders with the pore sizes (typically less than l0 μm) being similar to that of the original inter powder spacing. The total porosity in the majority of HIP specimens was estimated to be <3 vol% which is consistent with previous researcher (Murray & Dunan, 2006).

Figure 3(b) illustrates a typical backscattered image of the sample foamed at 1100 °C for 10 hours with the porosity being calculated to be 10.3 vol%. In this micrograph the dissolution of particles was evident with the tantalum and niobium particles having diffused and become indistinguishable. This result suggests that annealing or foaming at 1100 °C with a longer holding time may encourage additional alloying, even while the pressurised pores are causing the metal matrix to expand. Also noted in this micrograph was the presence of two distinct regions; a prominent lighter grey area representing β phase and a smaller dark area which represents α phase. From analysis of peak height ratios in these two regions by energy dispersive spectroscopy, it was estimated that the β phase comprised of a higher composition of β stabilising elements (ie. Nb, Ta, Zr) when compared to the α phase.

The development of α phase could be observed in samples foamed at higher temperatures (1225 and 1350 °C) as shown in figure 4. When foamed at

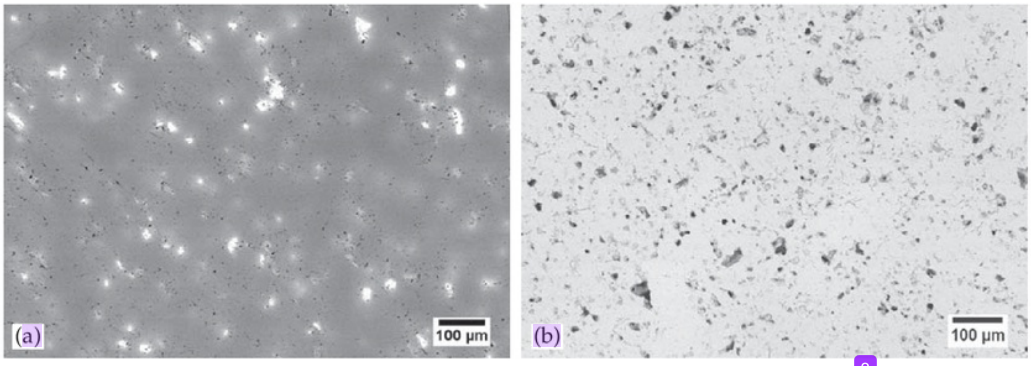

Figure 3: Backscattered electron image of titanium alloy specimen – (a) HIP at 1100 °C for 4 hours, and (b) foamed at 1100 °C for 10 hours.

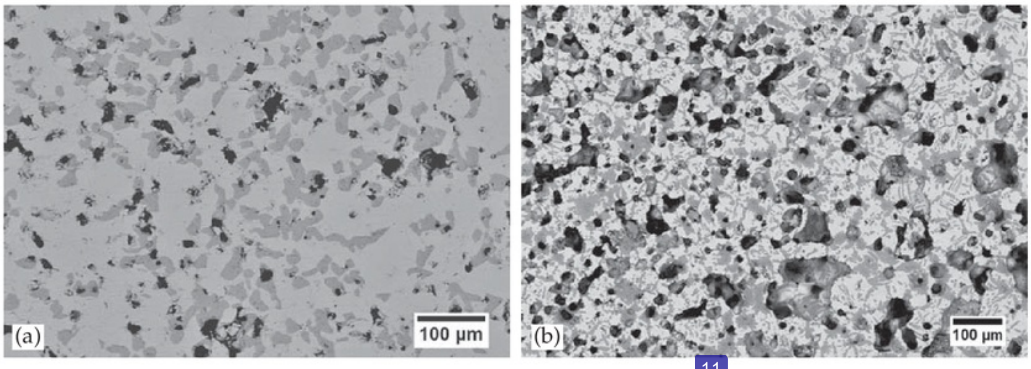

Figure 4: Backscattered scanning electron image of samples foamed at (a) 1225 °C and (b) 1350 °C.

1225 °C, the α phase, represented by the dark area, became larger; these areas appeared as α islands surrounded by β phase. When foaming at the highest temperature (1350 °C), the α phase continued to grow by forming α platelets within the β phase matrix along with further pore expansion. Thus, the microstructural analysis is in strong agreement with the XRD analysis. The pore morphology of the samples foamed at 1225 °C remained discrete with few coalesced pores and with only a small number of pores exceeding 44 μm in size (figure 4 (a)). In contrast to this, samples foamed at 1350 °C indicated the pores to have grown considerably larger with the porosity level achieving 38.5 vol% and a pore size of typically 20-100 μm; this was attributed to creep deformation of the metal and was found to increase with higher foaming temperatures. Rupturing of some side pore walls was observed, indicating that many pores had coalesced with multiple pores sometimes having become interconnected (figure 4(b)). The foaming rate is known to be suppressed if the pores expand through to the specimen surface due to escaping pressurised argon, while a rise in pore volume will also decrease the foaming rate as the driving force for further expansion will be reduced. According to previous studies, the optimal porosity and pore size of implant materials is in the range of 20-50 vol% (Thieme et al, 1999) and 50-125 μm (Itala et al, 2001), respectively. This fabricated porous titanium alloy achieved porosity levels of greater than 20 vol% and, together with the pore sizes mentioned earlier, suggests potential for biomedical applications.

Typical stress-strain curves for the samples foamed at 1100, 1225 and 1350oC have been presented in Figure 5 with a marked difference in stress-strain behaviour being noted. The typical curve for the sample foamed at 1100oC (Figure 5(a)) indicated a large amount of ductility in compression with three stages of deformation being apparent: elastic stage, plateau stage and densification stage. The samples were able to sustain compression strains of more than 35% without collapse. Figures 5(b) depicts a typical stress-strain response for the samples foamed at 1225oC with this curve being typical for ductile porous materials. In contrast to this, the curve shown in Figure 5(c) for a typical specimen foamed at 1350oC was characteristic of brittle failure. While the strength of this specimen (typically 790 MPa) was higher than that of the less porous specimens foamed at 1100 and 1225oC, the strain at maximum stress was significantly lower at generally less than 3%. The occurrence of an increase in brittleness for titanium alloys has previously been linked to the existence of oxygen in the porous metal (Jorgensen & Dunand, 2010).

The Young's modulus of the porous titanium alloys were calculated from the initial linear elastic region of the compressive stress-strain curves with the results from several specimens foamed at 1100, 1225 and 1350 °C being presented in figure 6 as a function of pore volume fraction.

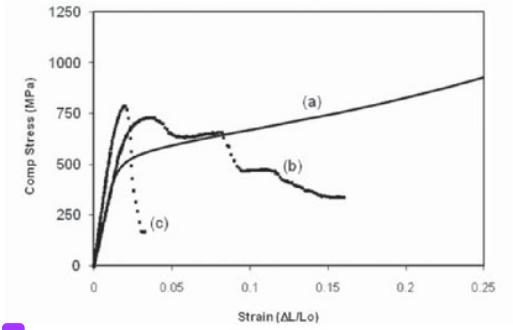

Figure 5: Typical compression stress-strain curves for the specimens foamed at (a) 1100 °C, (b) 1225 °C and (c) 1350 °C.

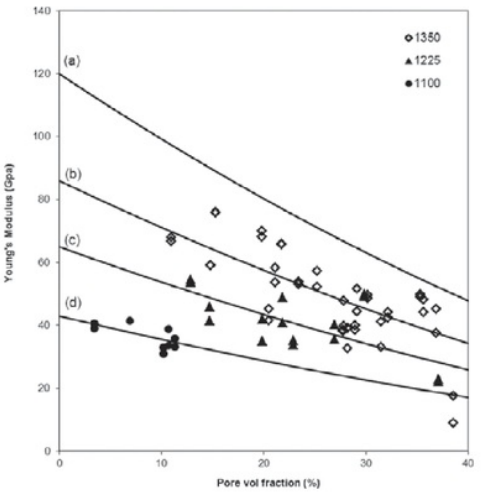

Figure 6: Influence of pore volume fraction on the elastic modulus of (a) fully dense titanium (theory), and foamed samples at 1350, 1225 and 1100 °C (marked) with their models (b), (c), (d), respectively.

All of the foamed samples exhibited a similar tendency in that the elastic modulus decreased with increasing pore volume fraction. The porous alloys foamed at 1100 °C showed the lowest values of elastic modulus, with a general increase in modulus as the foaming temperature increased, ie. 1225 and 1350 °C. As a comparison, the theoretical curves for fully dense pure titanium and the porous alloys foamed at 1350, 1225 and 1100 °C (based on a fully dense Young's modulus of 120 (Donachie, 1989), 85, 65 and 43 GPa, respectively; estimated from average values of the fully dense elastic modulus from the data points), have also been plotted (figure 6). The generally low values of stiffness in the samples foamed at 1100 °C was attributed to the increased presence of β phase, which is known to possess the lowest elastic modulus of the three phases, ie. β,

α and ω (Collings, 1984). As mentioned earlier, an increase in the foaming temperature increased the proportion of α phase, thus leading to an increase in the elastic modulus. The elastic moduli of the three sets of porous alloys, containing pore volume fractions in the range 3.5-38.5 vol%, were observed to vary between 9.1-76.2 GPa, thereby illustrating that a wide range of porosities and stiffnesses in beta stabilised titanium can be achieved from elemental starting powders. It should be noted that the range of elastic moduli encountered in the present investigation for porous titanium alloys included the typical range of values noted for nature bone (10-40 GPa) (Long & Rack, 1998). According to Erk et al (2008), the measured elastic modulus value can be estimated using the following model developed by Gibson & Ashby (1997):

$$\frac{E^*}{E_s} = \left(\frac{\rho^*}{\rho_s}\right)^n \quad (1)$$

where E^* and E_s are the Young's modulus of the porous and fully dense titanium alloys, respectively, and ρ^*/ρ_s is the relative density of the porous and fully dense titanium alloy, which is equivalent to 1 – pore volume fraction. n is a scaling exponent which is known to possess values between 1.8-2.2 (Ashby et al, 2000) with a value of n = 1.8, as reported by Erk et al (2008), being used in this work. While the data points followed the general trends in the theory curves predicted from equation (1), a significant amount of scatter was present within each foaming condition. This scatter was attributed to the presence of imperfections in the porous alloys such as irregular pore shapes, non-uniform pore sizes, and random pore size distributions, whereas the theory used by equation (1) is based on an idealised microstructure, eg. uniform cellular or pore shapes arranged in a cubic array.

4 CONCLUSIONS

Porous titanium alloys containing β stabilised elements with low toxicity, ie. Nb, Ta and Zr, have been successfully developed from the expansion of argon filled pores using elemental powder as starting materials. The porous titanium alloys were fabricated to achieve porosity levels and pore sizes of up to approximately 38.5% and 20-100 μm, respectively. Young's moduli values under compressive loading of the porous titanium alloys foamed at 1100, 1225 and 1350 °C were found to be in the range of 9.1-78.2 GPa. The presence of α phase, which increased with foaming temperature, was found to have a strong effect on increasing Young's modulus within the TiNbTaZr quaternary alloy under investigation. This porous titanium alloy is expected to be a promising candidate for low stiffness biocompatible implant materials.

ACKNOWLEDGEMENTS

Financial support provided by TPSDP, SPMU: Muhammadiyah University of Yogyakarta, Indonesia during the course of this work is greatly acknowledged. The authors also wish to thank the Australian Nuclear Science and Technology Organisation (ANSTO), Sydney for carrying out the HIP and foaming procedures.

REFERENCES

Ashby, M. F., Evans, A., Fleck, N. A., Gibson, L. J., Hutchinson, J. W. & Wadley, H. N. G. 2000, *Metal Foams: A Design Guide*, Butterworth-Heinemann.

Banumathy, S., Mandal, R. K. & Singh, A. K. 2009, "Structure of orthorhombic martensitic phase in binary Ti-Nb alloys", *Journal of Applied Physics*, Vol. 106, pp. 093518-1-093518-6.

Collings, E. W. 1984, *The Physical Metallurgy of Titanium Alloys*, Vol. 3, American Society for Metals, Ohio.

Donachie, Jr, M. J. 1989, *TITANIUM a Technical Guide*, 2nd edition, ASM International, Ohio.

Eisenbarth, E., Velten, D., Muller, M., Thull, R. & Breme, J. 2004, "Biocompatible of β-stabilizing elements of titanium alloys", *Biomaterial*, Vol. 25, pp. 5705-5713.

Erk, K. A., Dunand, D. C. & Shull, K. R. 2008, "Titanium with controllable pore fractions by thermoreversible gelcasting of TiH2", *Acta Materialia*, Vol. 56, pp. 5147-5157.

Gibson, L. J. & Ashby, M. F. 1997, *Cellular Solids: Structure and Properties*, 2nd edition, Cambridge University Press, Cambridge.

Hao, Y. L., Yang, R., Niinomi, M., Kuroda, D., Zhou, Y. L., Fukunaga, K. & Suzuki, A. 2002, "Young's modulus and mechanical properties of Ti-29Nb-13Ta-4.6 Zr in relation to martensite", *Metallurgical and Materials Transactions A*, Vol. 33, pp. 3137-3144.

Ikeda, M., Komatsu, S. Y., Sowa, I. & Niinomi, M. 2002, "Aging behaviour of the Ti29-Nb-13Ta-4.6Zr new beta alloy for medical implants", *Metallurgical and Materials Transactions*, Vol. 33A, pp. 487-493.

Itala, A. I., Ylanen, H. O., Ekholm, C., Karlsson, K. H. & Aro, H. T. 2001, "Pore diametre of more than 100 micrometre is not requisite for bone ingrowth in rabbits", *Journal of Biomedical Materials Research*, Vol. 58, pp. 679-683.

Jee, C. S. Y., Ozguven, N., Guo, Z. X. & Evans, J. R. G. 2000, "Preparation of high porosity metal foam",

Metalurgical and Materials Transactions, Vol. 31B, pp. 1345-1352.

Jorgensen, D. J. & Dunand, D. C. 2010, "Ti-6Al-4V with micro and macro pores produced by powder sintering and electrochemical dissolution of steel wires", *Materials Science and Engineering: A*, Vol. 527, pp. 849-853.

Kearns, M. W., Blenkinsop, P. A., Barber, A. C. & Farthing, T. W. 1987, "Manufacture of a novel porous materials", *Metals and Materials (Institute of Metals)*, Vol. 3, pp. 85-88.

Long, M. & Rack, H. J. 1998, "Titanium alloy in total joint replacement-a materials science perspectives", *Biomaterials*, Vol. 19, pp. 1621-1639.

Murray, N. G. D. & Dunand, D. C. 2004, "Effect of thermal history on the superplastic expansion of argon-filled pores in titanium: Part I kinetics and microstructure", *Acta Materialia*, Vol. 52, pp. 2269-2278.

Murray, N. G. D. & Dunan, D. C. 2006, "Effect of initial preform porosity on solid-state foaming of titanium", *Journal of Material Research*, Vol. 21, pp. 1175-1188.

Niinomi, M. 1998, "Mechanical Properties of biomedical titanium alloys", *Materials Science and Engineering A*, Vol. 243, pp. 231-236.

Oh, I. H., Nomura, N., Masahashi, N. & Hanada, S. 2003, "Mechanical properties of porous titanium compacts prepared by powder sintering", *Scripta Materialia*, Vol. 49, pp. 1197-1202.

Oppenheimer, S. 2007, "Processing and characterization of porous Ti-6Al-4V and NiTi", Dissertation of Doctor of Philosophy, Materials Science and Engineering Department, Northwestern University, Illinois, pp. 70-72.

Perl, D. P. & Brody, A. R. 1980, "Alzheimer's disease: X-ray spectrometric evidence of aluminum accumulation in neurofibrillary tangle-bearing neurons", *Science*, Vol. 208, pp. 297-299.

Rae, T. 1981, "The toxicity of metals used in orthopaedic prostheses: An experimental study using cultured human synovial fibroblasts", *Journal of Bone & Joint Surgery*, British Volume, Vol. 63, pp. 435-440.

Sakaguchi, N., Mitsuo, N., Akahori, T., Saito, T. & Furuta, T. 2004, "Effect of alloying elements on elastic modulus of Ti-Nb-Ta-Zr system alloy for biomedical applications", *Materials Science Forum*, No. 449-452, pp. 1269-1272.

Song, Y., Xu, D., Yang, R., Li, D., Wu, W. T. & Guo, Z. X. 1999, "Theoretical study of the effects of alloying elements on the strength and modulus of β-type bio titanium alloys", *Materials Science and Engineering A*, Vol. 260, pp. 269-274.

Taddei, E. B., Henriques, V. A. R., Silva, C. R. M. & Cairo, C. A. A. 2004, "Production of new titanium alloy for orthopaedic implants", *Materials Science and Engineering C*, Vol. 24, pp. 683-687.

Tang, X., Ahmed, T. & Rack, H. J. 2000, "Phase transformation in Ti-Nb-Ta and Ti-Nb-Ta-Zr alloys", *Journal of Materials Science*, Vol. 35, pp. 1805-1811.

Thieme, M., Wieters, K. P., Bergner, F., Scharnweber, D., Worch, H., Ndop, J., Kim, T. J. & Grill, W. 1999, "Titanium powder sintering for preparation of porous FGM destined as skeletal replacement implant", *Materials Science Forum*, No. 308-311, pp. 374-380.

Processing and properties of porous TiNbTaZr alloy for biomedical applications using the powder metallurgy route

ORIGINALITY REPORT

19%	%	19%	%
SIMILARITY INDEX	INTERNET SOURCES	PUBLICATIONS	STUDENT PAPERS

PRIMARY SOURCES

1	A W Nugroho, G Leadbeater, I J Davies. "Processing and properties of porous Ti-Nb-Ta-Zr alloy for biomedical applications using the powder metallurgy route", Australian Journal of Mechanical Engineering, 2015 Publication	8%
2	Aris W. Nugroho. "Processing of a porous titanium alloy from elemental powders using a solid state isothermal foaming technique", Journal of Materials Science Materials in Medicine, 10/20/2010 Publication	4%
3	"Proceedings of the 8th Pacific Rim International Congress on Advanced Materials and Processing", Springer Nature, 2016 Publication	1%
4	A W Nugroho, G Leadbeater, I J Davies. "Fabrication and characterization of the porous titanium alloy by argon filled pore expansion technique", IOP Conference Series: Materials	1%

Science and Engineering, 2018
Publication

5	Mervi Puska, Allan J., Pekka Vallittu. "Chapter 3 Polymer Composites for Bone Reconstruction", InTech, 2011 Publication	1%
6	Deshpande, V.. "Energy absorption of an egg-box material", Journal of the Mechanics and Physics of Solids, 200301 Publication	1%
7	M. BEERMAN. "Oscillatory instability and rupture in a thin melt film on its crystal subject to freezing and melting", Journal of Fluid Mechanics, 09/2007 Publication	1%
8	Hernández, Alexander Franco(Silva, Cosme Roberto Moreira da). "Avaliação do comportamento microestrutural e em fadiga da liga Ti-35Nb-7Zr-5Ta sinterizada e termicamente tratada", RIUnB, 2012. Publication	1%
9	"Review: titanium and titanium alloy applications in medicine", International Journal of Nano and Biomaterials, 2007 Publication	1%
10	Taddei, E. B, V. A. R Henriques, C. R. M Silva, C. A. A Cairo, and M. C. Bottino. "Ensaio de	1%

citotoxicidade e influÃªncia do tratamento de solubilizaÃ§Ã£o na microestrutura da liga Ti-35Nb-7Zr-5Ta para potenciais aplicaÃ§Ãµes ortopÃ©dicas", MatÃ©ria (Rio de Janeiro), 2007.
Publication

11	"TMS 2014: 143rd Annual Meeting & Exhibition", Springer Nature, 2016 Publication	1%
12	Yuhua Li, Chao Yang, Haidong Zhao, Shengguan Qu, Xiaoqiang Li, Yuanyuan Li. "New Developments of Ti-Based Alloys for Biomedical Applications", Materials, 2014 Publication	1%

Exclude quotes	On	Exclude matches	< 1%
Exclude bibliography	Off		